Journal of Advanced Research (2010) 1, 39–51

University of Cairo

Journal of Advanced Research

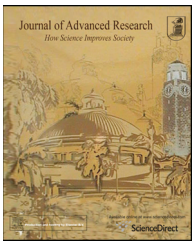

ORIGINAL ARTICLE

Multi-component fiber track modelling of diffusion-weighted magnetic resonance imaging data

Yasser M. Kadah [a,*], Inas A. Yassine [b]

[a] *Biomedical Engineering Department, Cairo University, Giza 12613, Egypt*
[b] *Lane Department of Computer Science and Electrical Engineering, West Virginia University, USA*

KEYWORDS

Diffusion imaging;
Magnetic resonance imaging;
Multi-tensor estimation;
Brain imaging

Abstract In conventional diffusion tensor imaging (DTI) based on magnetic resonance data, each voxel is assumed to contain a single component having diffusion properties that can be fully represented by a single tensor. Even though this assumption can be valid in some cases, the general case involves the mixing of components, resulting in significant deviation from the single tensor model. Hence, a strategy that allows the decomposition of data based on a mixture model has the potential of enhancing the diagnostic value of DTI. This project aims to work towards the development and experimental verification of a robust method for solving the problem of multi-component modelling of diffusion tensor imaging data. The new method demonstrates significant error reduction from the single-component model while maintaining practicality for clinical applications, obtaining more accurate Fiber tracking results.

Introduction

Among the unique features of magnetic resonance imaging (MRI) is its ability to characterise microscopic phenomena (such as diffusion) *in vivo* noninvasively [1]. In its most basic form, diffusion imaging attempts to characterise the manner by which water molecules within a particular location move within a given amount of time. Using a simple imaging sequence, it is possible to obtain a change of the MRI signal that is related to the diffusivity of water in a certain direction [2]. Given that such diffusivity varies with the geometry of the cellular space, it has an important value in discriminating between different tissue types as well as identifying abnormal variations in pathological states.

In order to avoid variations in diffusivity parameters with the positioning of the subject, a general characterisation of the diffusion process was introduced based on diffusion tensors. The basic techniques in diffusion tensor imaging (DTI) characterise the 3D diffusion in terms of a 3D Gaussian probability distribution [3]. Therefore, such representation is sufficient in terms of a 3×3 symmetric tensor, or the so-called "cigar-shaped" diffusion tensor representation. This tensor is usually computed using a 3D sampling of the b-space, or the space of the diffusion experiment *b*-values [4]. Recent studies have revealed several deviations from this simplified scenario. In this, a non-mono-exponential behaviour for the diffusion-

* Corresponding author. Tel.: +20 11 274 9681; fax: +20 23 573 6180.
E-mail address: ymk@k-space.org (Y.M. Kadah).
URL: http://ymk.k-space.org (Y.M. Kadah).

2090-1232 © 2009 University of Cairo. All rights reserved. Peer review under responsibility of University of Cairo.

Production and hosting by Elsevier

doi:10.1016/j.jare.2010.02.001

induced attenuation in brain tissue has been reported, whereby bi- or tri-exponential functions were found to better fit the data under high *b*-values [3]. Also, a two-compartment model for the diffusion in Fibers of the myocardium has been reported, with two fast and slow components assuming a slow-exchange process between the two [5]. Bi-exponential diffusion model has also been hypothesised to represent the intra- and extracellular components in tissues [6]. Variations of the apparent diffusion coefficient with diffusion time have also been reported and hypothesised to indicate restricted flow [7]. A two-tensor model for diffusion in the human brain has been reported in which the parameters of a mixture model composed of two weighted tensors representing fast and slow components are measured under high *b*-values [8]. Tuch et al. have noted that DTI measurements could only resolve imaging situations in which the white matter Fibers are strongly aligned [9]. They presented evidence from high angular resolution diffusion measurements to show that the diffusion process can be modelled as an independent mixture of ideal diffusion processes. They presented results for the case of a mixture of two diffusion tensors. The methodology used to obtain the mixture parameters was based on minimising an error function using gradient-descent technique. Beaulieu has discussed the sources causing anisotropic diffusion, including geometric, structural and pathological conditions [10]. This study concluded that the presence of such processes restricting diffusion in certain directions could be used to account for the measured anisotropy in DTI measurements. Frank has reported a method for identifying the anisotropy in high angular resolution diffusion-weighted (HARD) imaging data without computing the actual tensor [11]. Another study by the same author developed a methodology for characterising HARD data by decomposition into spherical harmonics [12]. This approach allowed several modes of diffusion to be decomposed into separate channels that are different from those for eddy current artefacts. He studied the case of two Fibers under different conditions and proposed an extension of his method to characterise multiple Fiber scenarios. Given the complexity of such situations and the limitations of defining spherical harmonics in terms of rotations only, this might not be practical in many cases. Basser and Jones have discussed the possibility of mixture modelling of diffusion [3]. Even though they indicated that this would present a more complete representation of the process, they argued that there are too many issues to be resolved before such modelling can be performed in practice. Their hypothetical discussion indicated that such modelling would require a large amount of data to enable the estimation of model parameters and would involve the computation of too many parameters.

Observing that the diffusion along nerve Fibers tends to be significantly larger than in other directions [13], Fiber directions were computed from diffusion tensor data. The basic idea was to eigen-decompose the diffusion tensor and use the eigenvector corresponding to the largest eigenvalue as the Fiber direction in a given pixel. This simplistic representation of the problem is often unsuitable for real data, where Fiber direction heterogeneity is common. Ambiguity arises in situations where the direction of the Fiber cannot be determined [14]. For example, in voxels where the estimated diffusion ellipsoid takes a disc shaped rather than a cigar shaped form, the tracking algorithms terminate, resulting in undesired disconnections in the resulting Fiber tracks. Poupon et al. have reported problems with the tracking results when crossing Fibers are encountered and suggested a regularisation strategy to solve this problem [15]. Other regularisation methods have also been reported [16,17]. The performance of such methods is still bound by the original single-tensor model limitations.

The goal of this work is to derive a methodology for multi-component Fiber tracking based on high angular resolution diffusion-weighted acquisitions. A compartmental model representing the physical make-up of imaging pixels is considered. Based on an analytical expression of apparent diffusion tensor, the mixture model parameters are calculated. Heterogeneity of components is allowed in the model by proposing a pixel model with multiple tensors instead of one under normal *b*-values. Hence, this model is different from the reported fast/slow component modelling, while alleviating the limitations of the previous single-tensor modelling.

Methodology

Problem formulation

The true diffusion-weighted signal from a single diffusion compartment is given by:

$$E(q_k) = \exp(-q_k^T \mathbf{D} q_k \tau), \tag{1}$$

where $E(q_k)$ is the normalised diffusion signal magnitude for the diffusion gradient wave-vector $q_k = \gamma \delta g_k$, γ is the gyromagnetic ratio, δ is the diffusion gradient duration, g_k is the kth diffusion gradient, τ is the effective diffusion time, and $\mathbf{D}$ is the apparent diffusion tensor. To model multiple compartments, we assume that the inhomogeneity consists of a discrete number of homogeneous regions, the regions are in slow exchange, and the diffusion within each region is Gaussian. Then, we can express the true diffusion-weighted signal as a finite mixture of Gaussian functions given as,

$$E(q_k) = \sum_{i=1}^{M} f_i \exp(-q_k^T \mathbf{D} q_k \tau). \tag{2}$$

Here, f_i is the volume fraction of component i, M is the number of components, and $\sum_{i=1}^{M} f_i = 1$. We can consider the problem of a voxel with two distinct components (without loss of generality). In this case, the number of unknowns to fully describe the model is 13 (two symmetric tensors and one partial volume ratio). In this case, the model takes the form,

$$E(q_k) = f_1 \exp(-q_k^T \mathbf{D}_1 q_k \tau) + (1 - f_1) \exp(-q_k^T \mathbf{D}_2 q_k \tau). \tag{3}$$

Unlike the problem of estimating a single tensor, the equations here are nonlinear but cannot be linearised by taking the natural logarithm of both sides. The attenuation equation for each tensor resembles a sample of a 3D Gaussian function with a covariance matrix equal to the diffusion tensor evaluated at a point determined by the diffusion gradient direction at a radius equal to the square root of the *b*-value. Hence, the problem of estimating multiple tensors becomes one of 3D Gaussian mixture modelling from samples determined by the diffusion gradient vector sampling. This estimation problem is nonlinear and therefore only iterative estimation methods have been proposed in the literature. Given the convergence issues associated with such methods and their generally high computational burden, a new practical strategy is needed to solve this problem. Note that for any given parameter estimation accuracy, there exists a finite number of possible solutions that are determined

by the *a priori* information about parameter ranges and the desired accuracy. Hence the problem of finding the solution to this problem amounts to a combinatorial optimisation problem. This means that a globally optimal solution can be found by exhaustive search or one of the more efficient random search strategies such as simulated annealing or genetic algorithms. Nevertheless, the computational effort involved in such techniques is prohibitive.

In this work, two new methods for estimating the tensors are developed and compared to the most widely cited method of using gradient descent, as proposed by Tuch et al. [9]. The effect of noise in the data (conventionally assumed to be due to the thermal noise in the MRI system electronics) on the solution is also studied. The diffusion time is assumed to be the same for different gradient vector orientations having the same b-value. Unlike previous work in this field, no assumptions will be made about the diffusion tensor to maintain generality and practicality of the solution.

The gradient-descent method

The traditional method for solving Gaussian mixture problems of this type is the expectation maximisation (EM) algorithm. However, given the need to solve the mixture problem with physiological constraints on the eigenvalues, the EM algorithm is no suitable for handling such hard constraints. Therefore, a gradient-descent scheme is employed with multiple random starting points to solve the mixture model by solving the eigenvectors and volume fractions that give the lowest error between the predicted and observed diffusion. The eigenvalues of the individual tensors are either specified *a priori* or restricted to a particular range in order to prevent the algorithm from over-fitting with physiologically-meaningless eigenvalues. Multiple random starting points were utilised to avoid getting trapped in local minima given the non-convex search space of the problem. Approximately half of the iterations found the global minimum. In Tuch et al. [9], the problem is assumed to be that of resolving white matter crossing Fibers. Hence the eigenvalues for white matter were specified *a priori* to be $(\lambda_1, \lambda_2, \lambda_3) = (1.5, 0.4, 0.4)$ $\mu m^2/ms$ based on the reported normal values. This is a clear limitation of this technique given the variability of such values within normal subjects, in addition to the failure to model situations where grey matter or cerebrospinal fluid are involved. The eigenvalues were preset in order to prevent the individual tensor fits from assuming oblate forms. The error function to be minimised is given as

$$x = \sum_k (\hat{E}(q_k) - E(q_k))^2 = \sum_k \left(\sum_j f_j \hat{E}_j(q_k) - E(q_k) \right)^2. \quad (4)$$

Here $\hat{E}$ is the predicted diffusion signal based on the multi tensor model, $\hat{E}_j(qk)$ is the predicted diffusion signal from compartment j (Eq. (1)) with volume fraction f_j, and E is the observed diffusion signal. To ensure that the volume fractions are properly bounded ($f_i \in [0, 1]$) and normalised such that their sum is equal to unity, the volume fractions are calculated through the soft-max transform [9].

$$f_j = \frac{\exp \eta_j}{\sum_i \exp \eta_i}. \quad (5)$$

The tensors $\mathbf{D}_j$ are parameterised in terms of the Euler angles α_j^i. The derivative with respect to the Euler angles is given by,

$$\frac{\partial x}{\partial \alpha_j^i} = -\sum_k (\hat{E}(q_k) - E(q_k)) f_i \hat{E}_j(q_k) q_k^T \left(\frac{\partial \mathbf{R}_j}{\partial \alpha_j^i} \Lambda_j \mathbf{R}_j^T + \mathbf{R}_j \Lambda_j \frac{\partial \mathbf{R}_j^T}{\partial \alpha_j^i} \right) q_k^T, \quad (6)$$

where $\mathbf{R}_j$ is the column matrix of eigenvectors and Λ_j is the diagonal matrix of eigenvalues for tensor $\mathbf{D}_j$. The gradient with respect to the volume fraction parameters is,

$$\frac{\partial x}{\partial \eta_i} = \frac{\exp \eta_i}{(\sum_i \exp \eta_i)^2} \sum_k \left[(\hat{E}(q_k) - E(q_k)) \times \sum_i (1 - \delta_{ij})(\hat{E}(q_k) - E(q_k)) \exp \eta_i \right], \quad (7)$$

where $\delta^{ij} = 1$ when $i = j$, and 0 otherwise.

The differential equation modelling technique

In this new method, we observe that the measurements in diffusion tensor imaging are usually obtained for uniformly distributed values of b. Recalling that the attenuation values are direct functions of the square root of b, Eq. (3) can be simplified for this case such that [21]

$$E(b) = f_1 \exp(-b/\tau_1) + (1 - f_1) \exp(-b/\tau_2), \quad (8)$$

where $\tau_i = 1/(q_k^T D_i q_k)$. As a result of this formulation, the problem is now transformed into the parameter estimation of exponentially decaying signals. Hence we can describe the system using a homogeneous second-order differential equation in the form

$$E''(b) + a_1 E'(b) + a_2 E(b) = 0, \quad (9)$$

where

$$E'(b) = -\frac{f_1}{\tau_1} \exp(-b/\tau_1) - \frac{(1 - f_1)}{\tau_2} \exp(-b/\tau_2), \quad (10)$$

and

$$E''(b) = \frac{f_1}{\tau_1^2} \exp(-b/\tau_1) + \frac{(1 - f_1)}{\tau_2^2} \exp(-b/\tau_2). \quad (11)$$

Since the values of $E(b)$ are available for several values of b, its first- and second-order derivatives can be obtained numerically from these values using the forward or central numerical differentiation formulas or using the frequency domain method using the differentiation property of the Fourier transform. In our simulations, using the central numerical differentiation we can formulate a linear system to estimate the coefficients of the differential equation as,

$$\begin{bmatrix} E'(b_1) & E(b_1) \\ E'(b_2) & E(b_2) \\ \vdots & \vdots \\ E'(b_n) & E(b_n) \end{bmatrix} \begin{bmatrix} a_1 \\ a_2 \end{bmatrix} = - \begin{bmatrix} E''(b_1) \\ E''(b_2) \\ \vdots \\ E''(b_n) \end{bmatrix}. \quad (12)$$

Once the coefficients of the equations are computed, the second-degree polynomial characteristic equation is solved to obtain the roots corresponding to the exponential factors. Then it is straight forward to compute the magnitudes from solving the linear equations obtained by substituting the estimated variances.

Projection pursuit based method

In this second new method, the problem of estimating the composition of a voxel with two distinct components is considered (without loss of generality for multiple components). As discussed previously, the equations are nonlinear and therefore only iterative techniques can be utilised. We observe that the attenuation equation for each tensor resembles a sample of a 3D Gaussian function with a covariance matrix equal to the diffusion tensor evaluated at a point determined by the diffusion gradient direction at a radius equal to the square root of the *b*-value. Hence the problem of estimating multiple tensors becomes one of 3D Gaussian mixture modelling from samples determined by the diffusion gradient vector sampling.

To overcome this difficult estimation, we propose the use of projection pursuit regression (PPR), a robust statistical tool that allows the estimation of such mixture models [18,19]. Instead of attempting the solution in the high dimensional space of this problem, PPR projects the problem into a number of 1D problems and then synthesises the solution to the original problem space [20]. Moreover, the problem can be simplified further by utilising a sampling strategy that converts the problem into the sum of two exponentials. This problem is solved using a robust strategy in which the exponential decay constants are estimated using exhaustive search and the magnitude functions are estimated using a linear system solution based on the choice of the decay constants. Given that the range of decay constants for human applications is rather limited, this strategy has superior speed to nonlinear least-squares methods while offering the global solution to the problem. Once the 1D model is estimated, it can be used to provide an equation for each diffusion tensor separately as identified by its partial volume ratio. For example, we identify the components with the larger partial volume ratio as component 1 in all projections and utilise such projections to reconstruct its tensor in the same way the single-tensor method works. Following this, the second tensor is computed based on projections with second largest partial volume ratio and so on for other components (if existing). The computed tensors are used to compute a new estimate of the component partial volume ratios based on the whole data set rather than each projection separately. Given that these ratios are affected by noise, the

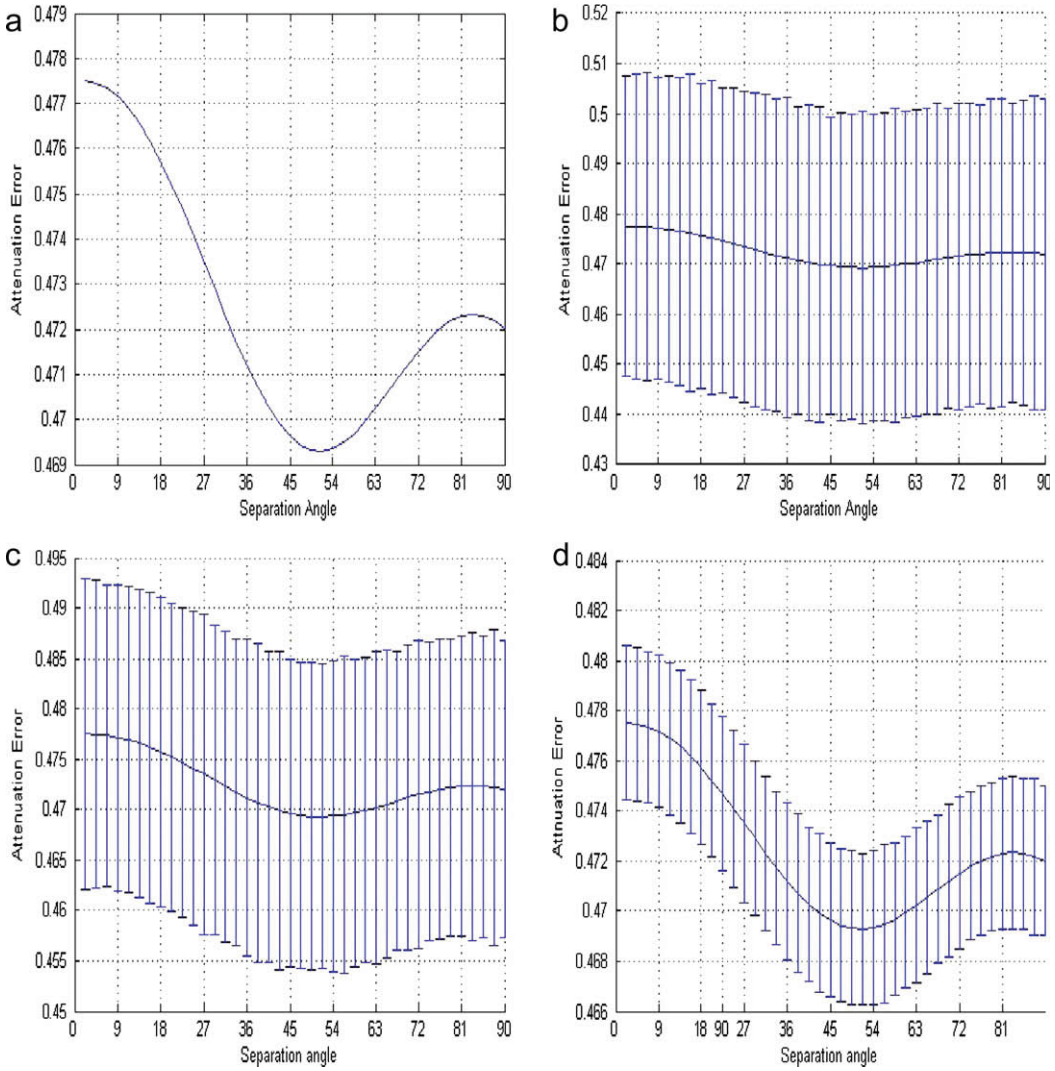

Figure 1 Estimated error in case of 12 gradient directions using the gradient-descent algorithm at different SNR values ((a) no noise, (b) 25 dB, (c) 35 dB, (d) 45 dB).

estimation process is started again with this new estimate plugged in for all projections and a new solution is estimated. This process is repeated until the partial volume ratio stabilises. In the general case of N-tensor model, the same procedure is followed at a computational cost that varies linearly with N.

The NMR signal attenuation due to diffusion when applying a gradient defined by the direction $\vec{x}$ is given by

$$E(\vec{x}) = \exp(-\pi \cdot \vec{x}^T \cdot D \cdot \vec{x}) \tag{13}$$

Here D is the diffusion tensor and $\vec{x} \equiv \sqrt{b/\pi} \cdot \vec{u}$ with a unit vector $\vec{u}$ in the direction of the gradients at an applied b-value of b. In order to proceed with the projection pursuit strategy, we must to be able to relate the characteristics of the diffusion tensor D to the one-dimensional projection of this function at an arbitrary direction. To compute this projection, we start with a 3D Gaussian function perfectly aligned with the coordinate axes and apply the rotation transformation to obtain the general formulation of the problem. Then, we utilise the projection-slice theorem to simplify the derivation of the projection integral. We start with the simplest form of the diffusion attenuation, defined as

$$\begin{aligned} E(\vec{x}) &= E([x \quad y \quad z]) \\ &= \exp\left(-\pi \cdot [x \quad y \quad z] \cdot \begin{bmatrix} \lambda_1 & 0 & 0 \\ 0 & \lambda_2 & 0 \\ 0 & 0 & \lambda_3 \end{bmatrix} \cdot \begin{bmatrix} x \\ y \\ z \end{bmatrix}\right) \\ &= \exp(-\pi \cdot \vec{x}^T \Lambda \vec{x}) \end{aligned} \tag{14}$$

The Fourier transformation of this function is given by

$$\begin{aligned} \Im\{E(\vec{x})\} &= \exp\left(-\pi \cdot [f_x \quad f_y \quad f_z] \cdot \begin{bmatrix} 1/\lambda_1 & 0 & 0 \\ 0 & 1/\lambda_2 & 0 \\ 0 & 0 & 1/\lambda_3 \end{bmatrix} \cdot \begin{bmatrix} f_x \\ f_y \\ f_z \end{bmatrix}\right) \\ &= \exp(-\pi \cdot \vec{f}^T \Lambda^{-1} \vec{f}^T). \end{aligned} \tag{15}$$

Here, we used the separability property to derive the 3D Gaussian Fourier transformation given the 1D transformation result. Consider now a diffusion tensor in a general direction given by

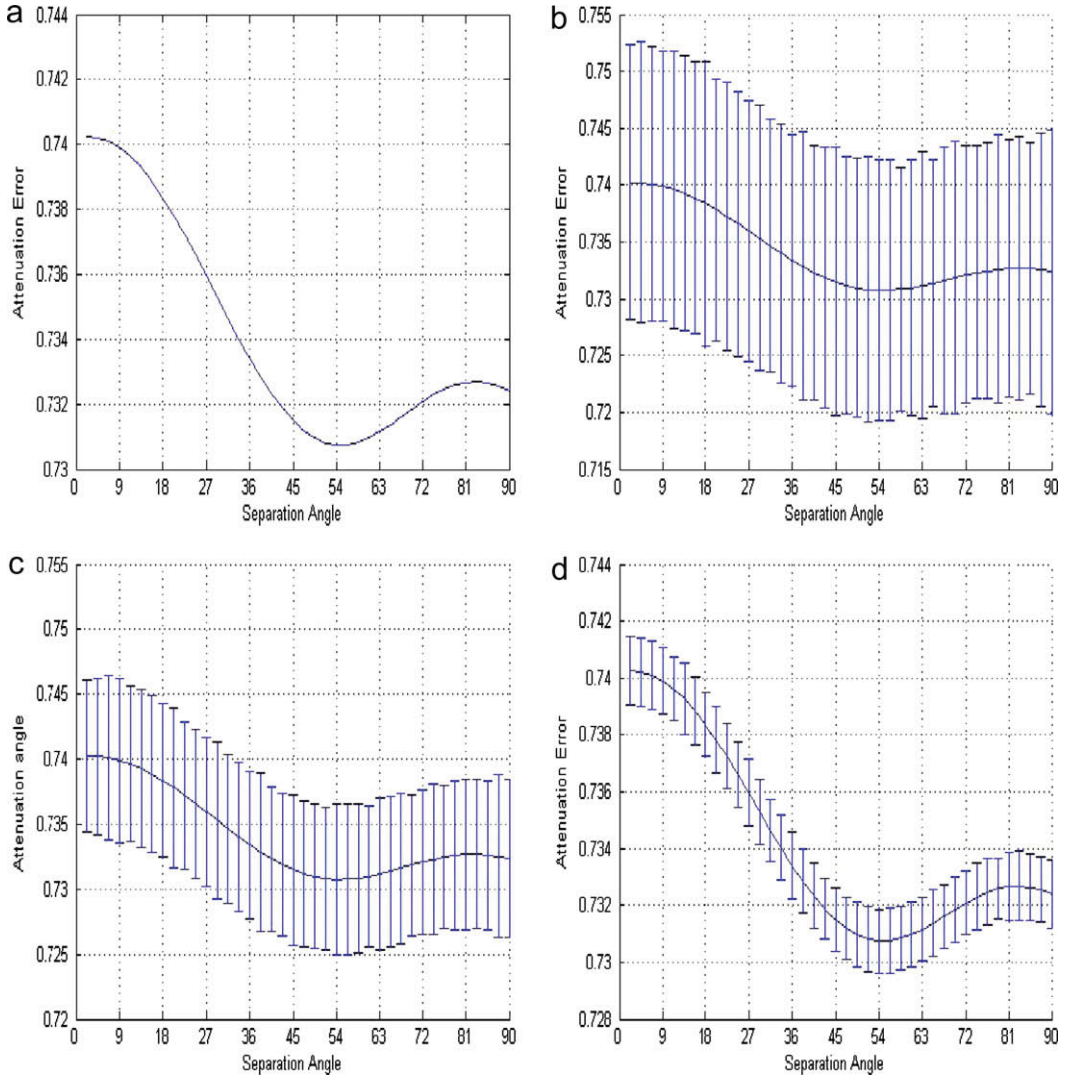

Figure 2 Estimated error in case of 30 gradient directions using the gradient-descent algorithm at different SNR values ((a) no noise, (b) 25 dB, (c) 35 dB, (d) 45 dB).

$$D = R^T \Lambda R, \tag{16}$$

where R is an orthogonal transformation. The Fourier transformation of this general case is given by

$$\Im\{E(\vec{x})\} = \exp(-\pi \cdot \vec{f}^T R^T \Lambda^{-1} R \vec{f}^T). \tag{17}$$

From the projection-slice theorem, the projection along a particular direction corresponds to a slice in the Fourier domain. Suppose that we would like to obtain the projection along the line that makes angles (θ, ϕ, φ) with the coordinate axes, respectively. We first notice that two angles are only sufficient to fully describe the required rotation given that the summation of the squares of the cosines of the three angles is equal to unity. To simplify the computation of the slice line (representing the Fourier transformation of the projection in the spatial domain), we apply a rotational transformation corresponding to the reverse of the line angle to align this line along the f_x axis. This rotation is computed as

$$A(\theta,\phi) = \begin{bmatrix} \cos\theta & -\sin\theta & 0 \\ \sin\theta & \cos\theta & 0 \\ 0 & 0 & 1 \end{bmatrix} \cdot \begin{bmatrix} 1 & 0 & 0 \\ 0 & \cos\phi & -\sin\phi \\ 0 & \sin\phi & \cos\phi \end{bmatrix} = \begin{bmatrix} \cos\theta & -\sin\theta\cos\phi & \sin\theta\sin\phi \\ \sin\theta & \cos\theta\cos\phi & -\cos\theta\sin\phi \\ 0 & \sin\phi & \cos\phi \end{bmatrix}. \tag{18}$$

Hence the line slice can be given as

$$\text{Slice} = \exp\left(-\pi f_x^2 [\cos\theta \quad -\sin\theta\cos\phi \quad \sin\theta\cos\phi\,] D^{-1} \times \begin{bmatrix} \cos\theta \\ -\sin\theta\cos\phi \\ \sin\theta\cos\phi \end{bmatrix} \right) = \exp(-\pi \cdot f_x^2 \cdot \sigma^2). \tag{19}$$

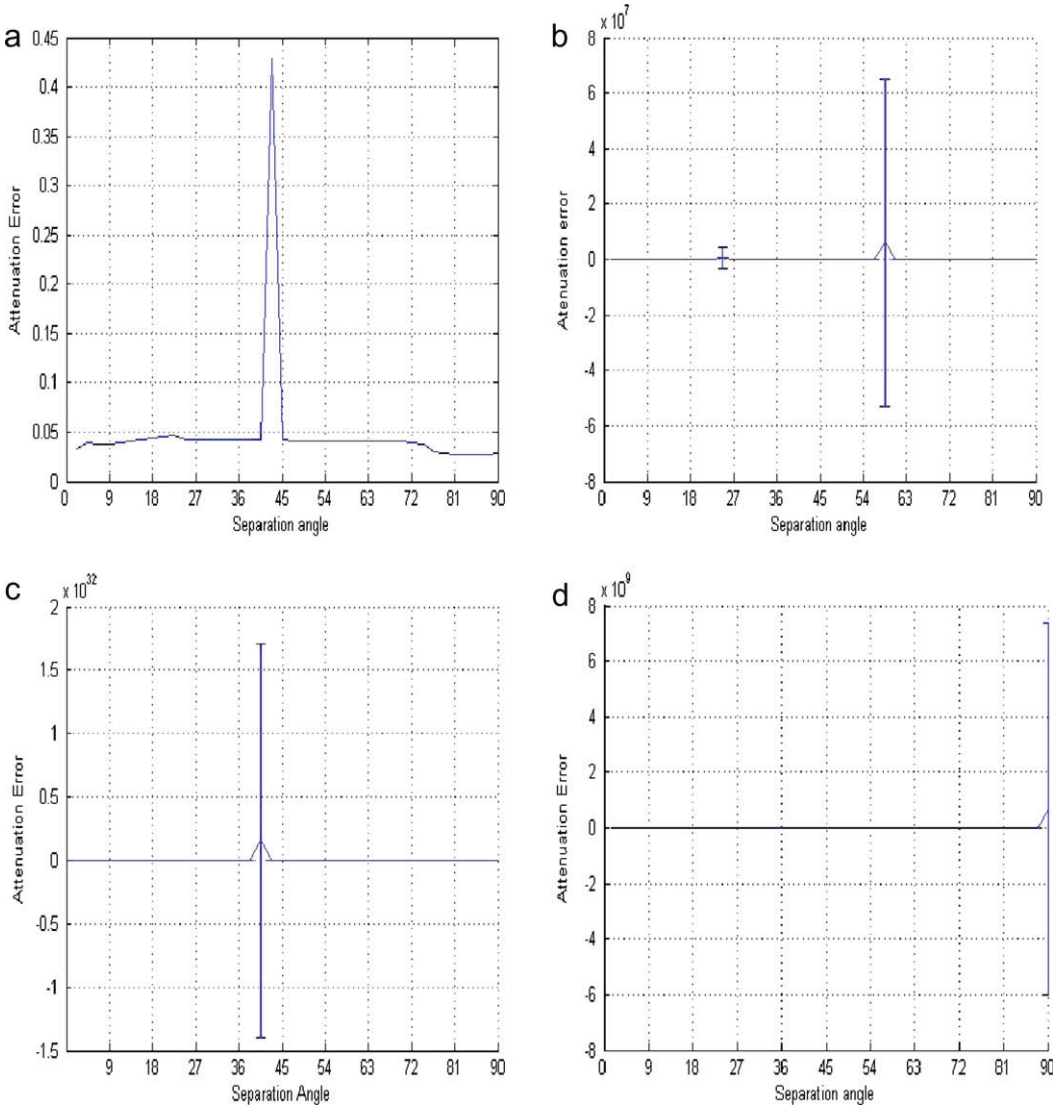

Figure 3 Estimated error in case of 12 gradient directions using the differential equation modelling technique at different SNR values ((a) no noise, (b) 25 dB, (c) 35 dB, (d) 45 dB).

The projection in the spatial domain can be given as

$$\text{projection} = \exp(-\pi \cdot x^2/\sigma^2). \tag{20}$$

Hence if we measure the variance σ^2 of the projection function along at least six directions, we can directly compute the inverse of the diffusion tensor and subsequently the diffusion tensor. Assuming a two-component model without loss of generality, the projection along any given direction can be given as

$$p(x) = \alpha_1 \cdot \exp(-\pi x^2/\sigma_1^2) + \alpha_2 \cdot \exp(-\pi x^2/\sigma_2^2). \tag{21}$$

Here the relative amplitudes are given by α_1 and α_2, and the variances are generally different for both components and vary with projection direction. The x value is known and can be computed given the b-value and the direction of diffusion gradients. The 1D component estimation problem amounts to the estimation of α_1, α_2, σ_1 and σ_2 given $p(x)$. Notice that the component amplitudes are the same between projections. This property will be used to aid in the labelling of components among different projections. As discussed before, this estimation problem is nonlinear and needs an iterative estimation method to obtain the solution. Here, we combine exhaustive search and least-squares estimation to obtain a faster implementation while maintaining the robustness and global optimality. In particular, instead of attempting to find all parameters by exhaustive search, we limit this strategy to those parameters of more importance in terms of accuracy and compute the remaining ones using least-squares estimation. This is implemented as follows:

Step 1. Take the variances to be the parameters estimated by exhaustive search while the partial volume ratios are estimated from them by least squares.

Step 2. Generate a list of possible values for the variances within the range from 0 to the maximum eigenvalue of the diffusion tensors of interest with the desired accuracy as the step.

Step 3. Plug in values for the variances in the equation from the list and compute the least-squares solution to the partial volume ratios for such values and compute the value of the residual error with such values plugged in.

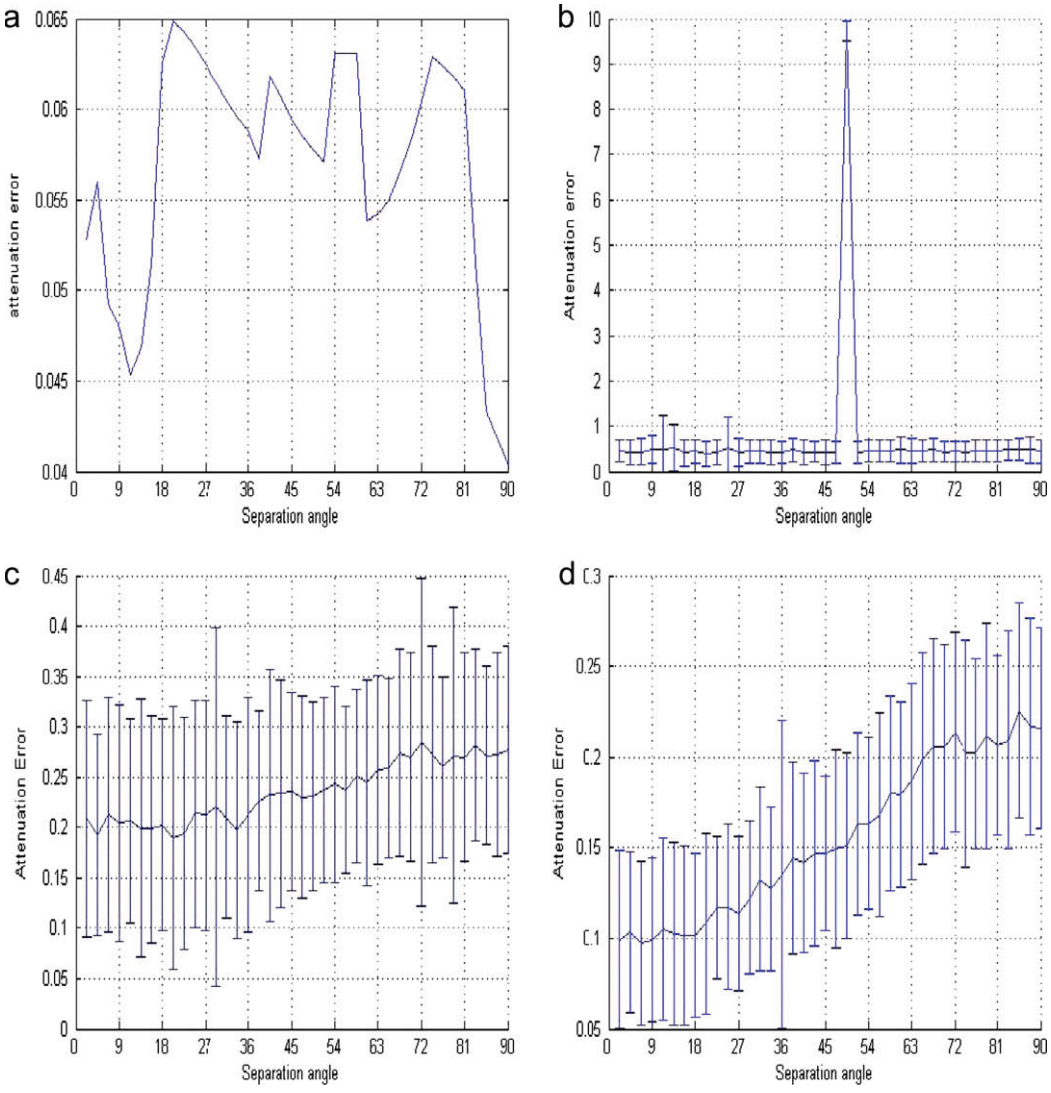

Figure 4 Estimated error in case of 30 gradient directions using the differential equation modelling technique at different SNR values ((a) no noise, (b) 25 dB, (c) 35 dB, (d) 45 dB).

Step 4. Loop all possible variance values in the list and repeat step 3 and find the combination of values that generate the lowest error. Consider such combination to be the solution.

This method allows an order of magnitude saving in computation time while providing a solution with sufficient accuracy. Once the individual component estimates from projections are computed, the projections of each component can be used to estimate the component tensor as in the single-tensor case. One problem arises because of component labelling. The basic assumption of the model that the partial volume ratios remain the same in projections may not be practical given the superimposed noise and other sources of error in DTI. In other words, partial volume ratios from different projections are slightly different in practice. To solve this problem, an initial labelling is obtained whereby the first component is calculated from the projection components having the larger partial volume ratio, while the second component is calculated from the components with the smaller one. Once the two tensors are computed using this strategy, a least-squares estimate for the partial volume ratios is computed while imposing the constraint of unit summation upon their values. Following this, the calculated values are used in a second iteration of the procedure above to update the projection variances while imposing the same partial volume ratios obtained from the first iteration. A second estimate of the partial volume ratios is computed at the end of the second iteration and this process is repeated until estimates from two successive iterations differ by a predetermined tolerance. In this case, the estimates represent the global solution that is not biased by error within individual projections.

It should be noted that the extension of this method to multiple exponentials is straightforward. The computational complexity depends linearly on the number of components. We still gain the separation between the problems of estimating the variances and the magnitudes. Moreover, the same direct magnitude estimation method can still be applied in this case once

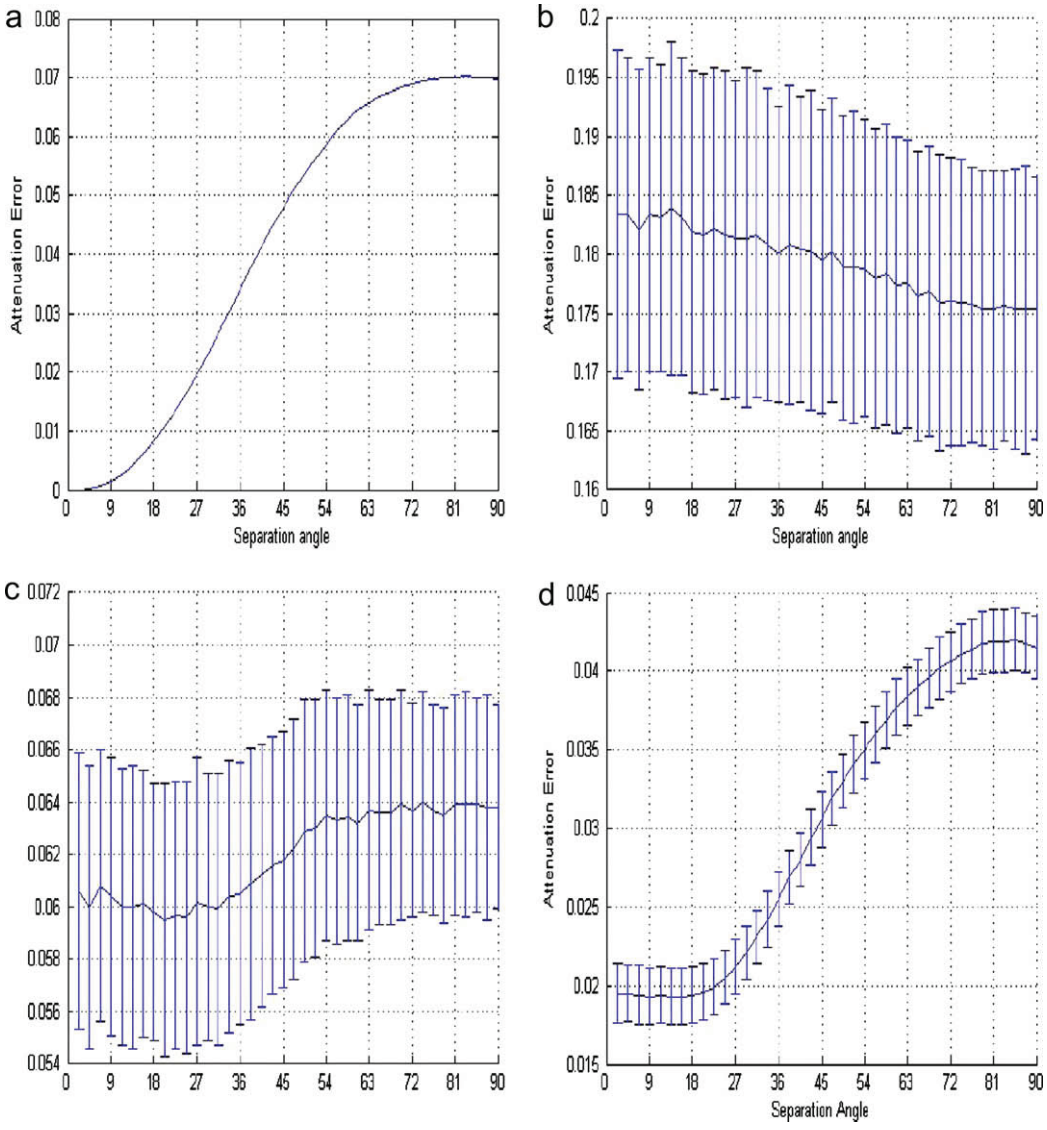

Figure 5 Estimated error in case of 12 gradient directions using the projection pursuit based method at different SNR values ((a) no noise, (b) 25 dB, (c) 35 dB, (d) 45 dB).

the roots are calculated. This can reduce the complexity dramatically. It should be noted, however, that the problem of two-component modelling will be addressed in the experimental verification phase since this is a problem of interest for practical applications where the presence of more than two significant components within a voxel is not likely [9,14].

Continuing to the simpler multi-exponential model, the problem of determining the best directions for projecting the

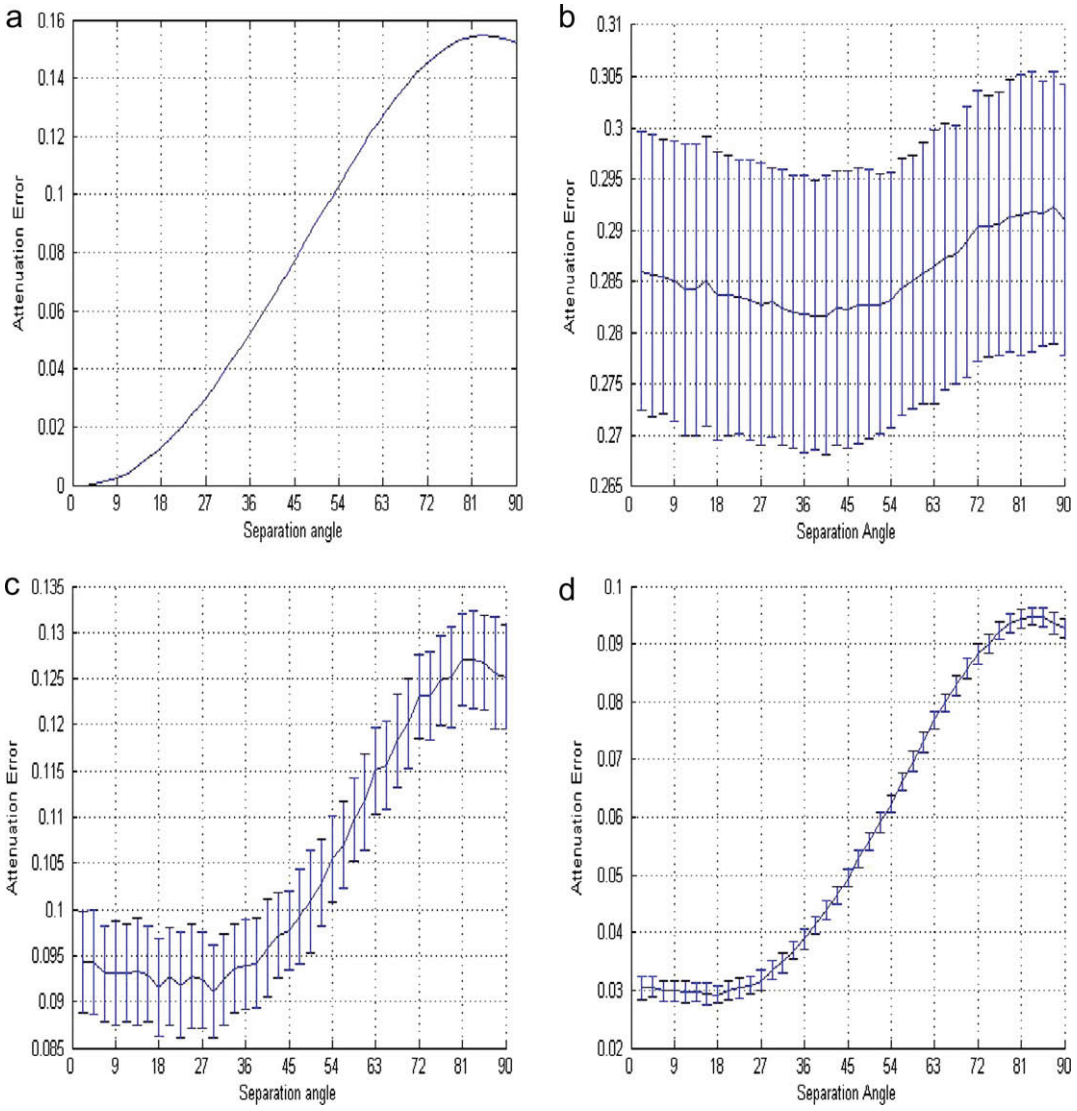

Figure 6 Estimated error in case of 30 gradient directions using the projection pursuit based method at different SNR values ((a) no noise, (b) 25 dB, (c) 35 dB, (d) 45 dB).

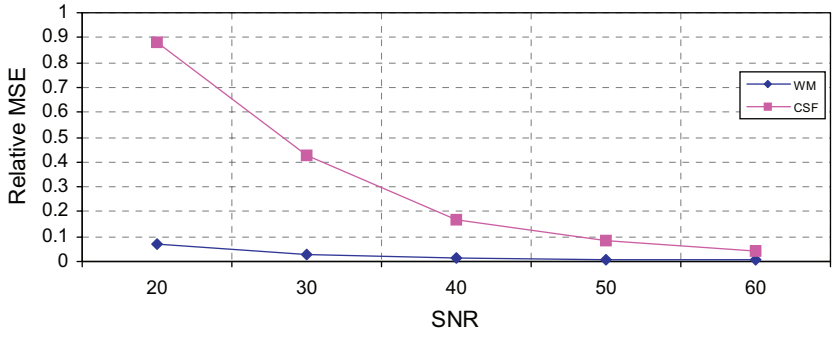

Figure 7 Monte Carlo simulations for the effect of noise on the multi-component model estimation.

multi-component model can be addressed similarly to the above. Instead of seeking the directions representing the maximum non-Gaussianity as in the original formulation of the PPR, we now see those directions representing the sharpest difference between the exponential decay constants. An excellent direction index for this purpose is the quantity under the square root in the second-degree characteristic polynomial root formula. Observing that this quantity is zero for equal roots and gets larger as the roots separate, the maximisation of this index provides a more efficient alternative to the kurtosis or other higher order moment optimisation in the original Gaussian mixture model.

Experimental verification

To evaluate the new methods and compare them to the previous method, two sets of experiments were conducted. The first conducted computer simulations to assess the accuracy of model estimation of the different methods under different signal-to-noise (SNR) values and voxel compositions. The second set of experiments applied the methods to real data sets obtained from a normal human volunteer.

The computer simulation was conducted on a DELL personal computer with a Pentium 4 processor with clock speed of 2.4 GHz with 512 MB of memory running the IDL scientific software package (Research Systems, Inc.). The developed simulation programs generated simulated two-tensor data sets based on the problem formulation above at different numbers of diffusion gradients and directions and the methods were implemented to estimate the tensors. The simulation parameters used were as follows: the acquisition of a cubic volume of size $8 \times 8 \times 8$ voxels that fully covered the 3D extent of the diffusion attenuation. The data were projected onto a number of directions that uniformly sampled the space where these directions were taken to be the same as those used in real DTI acquisition; namely as 12 or 30 directions.

Experimental results were also obtained from data sets collected from a normal human volunteer on a 3T Siemens Trio system (Siemens Medical Systems, Germany) using a double spin-echo sequence with 8 *b*-values spanning the range [0,1500] at 12 and 30 directions. Both scans were repeated 4 times to investigate the effect of SNR.

The total scan time for the 12-direction scan was 12 min while it was approximately 30 min for the 30-direction scan.

Results and discussion

Figs. 1 and 2 show the estimation error using the gradient-descent algorithm for different SNR values and numbers of gradient directions. The error in estimation is shown to be high and appears to decrease slowly with higher SNR. It is also clear that there is no deviation in estimates at low and high SNR. Figs. 3 and 4 show the estimation error using the differential equation modelling technique. The error in estimation and the standard deviation decreases with the increase of the SNR. It is also clear that instability in estimation occurs with 12 gradient directions, although they have better estimation than 30 gradient directions when there is no noise. The estimation error appears significantly less in this technique than the gradient-descent method. Figs. 5 and 6 show the estimation error when using the projection pursuit based method. The 12 gradient directions results show the least mean square error. The reason for this might be related to the fact that the condition number of the problem for the particular number of gradient directions, which was 1.00 for 12 gradient directions, and slightly higher (around 1.02) for 30 gradient directions. Comparing the three different techniques, the error in the projection pursuit based method was better than both differentiation and gradient algorithms. Therefore, we elected to focus on that method for further analysis.

Instead of selecting a few directions in the original PPR formulation, all directions were taken into consideration with a weighting corresponding to the model error. Also, within each 1D estimation procedure, a regularisation step was implemented to verify that the partial volume ratio of all components is above a certain threshold value. This is necessary since it is likely that the component projections may have similar decay at some directions resulting in an ill-conditioned solution. The simulation results of a model composed of both white matter (WM) and CSF are shown in Fig. 7. Notice that

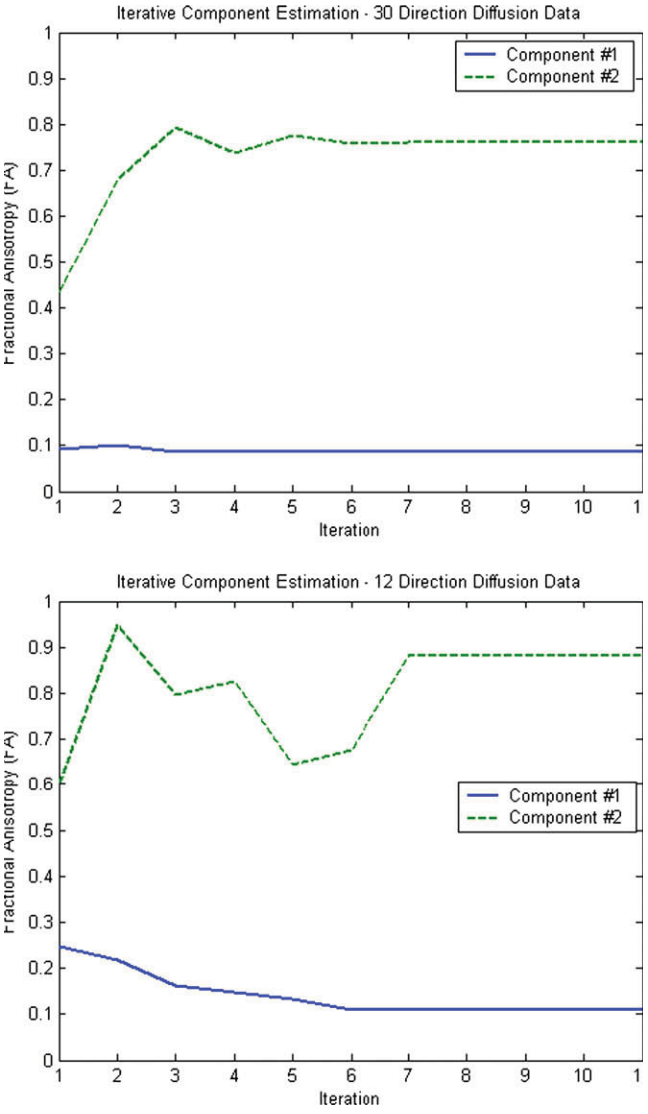

Figure 8 Illustration of the solution convergence in two-tensor modelling as represented by the FA of components for both 12-direction and 30-direction data acquisition schemes.

for SNR above 50 dB the estimation error of the tensors is below 10%. The model estimation procedure for each voxel was performed within an average of less than 1 sec (based on a 2.4 GHz P4 computer with 512 MB RAM), which is reasonable for practical purposes.

The iterative estimation procedure is illustrated for a single voxel in Fig. 8, where the fractional anisotropy [1] is computed for both components of the two-tensor model to illustrate the convergence in both the 12- and 30-direction acquisitions. The convergence appears to occur within a few iterations. The

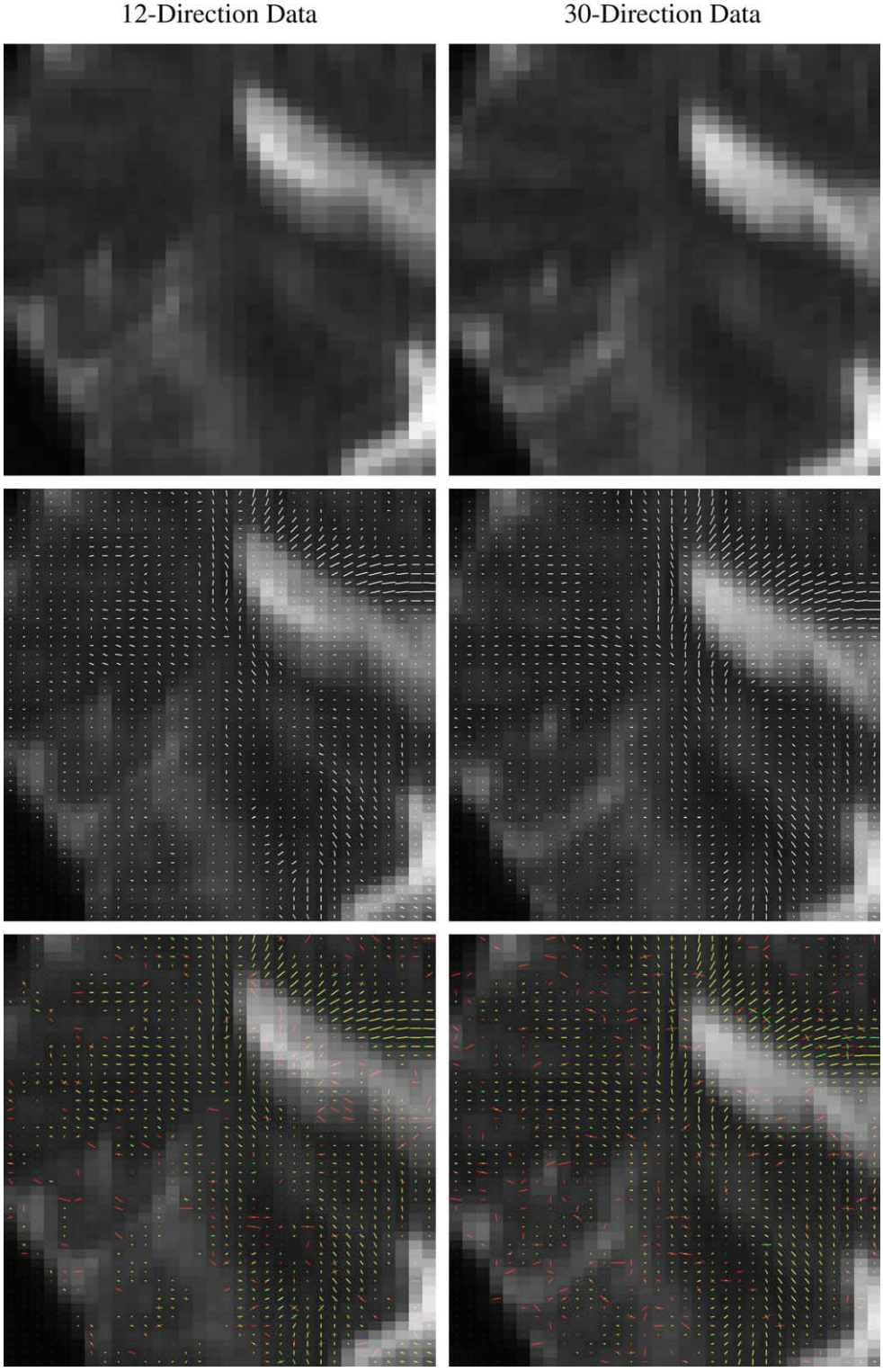

Figure 9 Detailed results from real data for 12-direction (left) and 30-direction (right) acquisitions with anatomical images (top), one-tensor model (middle) and two-tensor model (bottom).

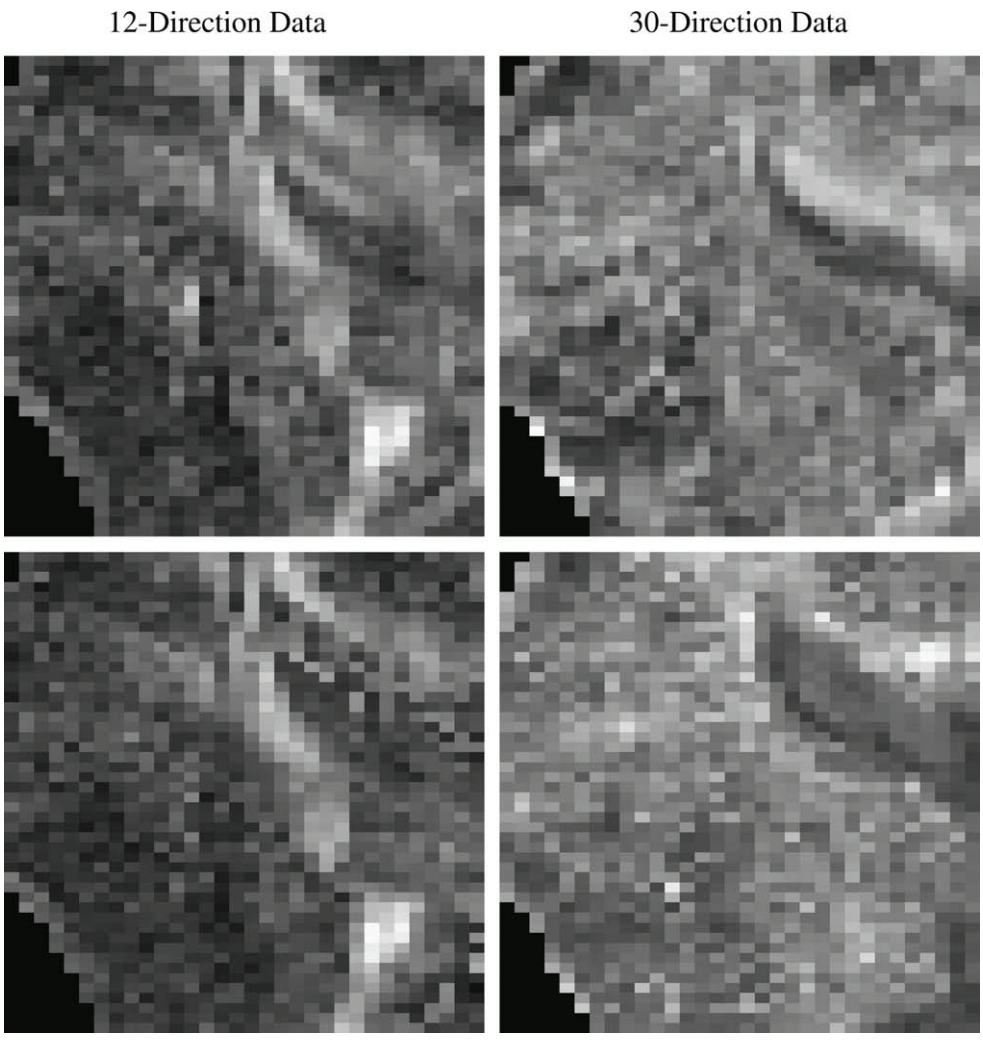

Figure 10 Estimation error maps from real data for 12-direction (left) and 30-direction (right) acquisitions with one-tensor model error map (top) and two-tensor model error map (bottom). A significant reduction in errors is visible in regions where partial voluming is likely to occur such as near CSF.

tensor field results from experimental data with 30 diffusion gradient directions and 4 averages are shown in Figs. 9 and 10, where the new method is compared to the one-tensor model visually and using an error measure of the fitting accuracy. The tensors are drawn in such a way as to show CSF tensors as points and white matter tensors as lines. As can be shown, the areas that show partial voluming at the interfaces of the CSF areas show significant improvement in model error when the two-tensor model is used. The average reduction in model error over the whole ROI was 30.1% for the 30-direction data set and 8.9% for the 12-direction data set (individual voxels exhibit error rates that are up to 80% lower in some cases).

It should be noted that the results of this work provide a significant improvement over existing methodologies whereby the assumptions about the tensors to be estimated are more practical and the solution itself is robust under a practical range of signal-to-noise ratios, while keeping the computation time lower. With the encouraging results obtained, several applications should be addressed to verify the clinical utility of the new method. Examples include the removal of the effect of CSF contamination in both white matter and gray matter voxels and the ability to resolve crossing Fibers.

In spite of the visible improvement in residual error obtained with the new model, it is important to address several issues related to the regularisation of the model to avoid erroneous interpretation of the results. For example, a threshold must be set for the partial volume ratio below which the component is discarded as nuisance. This can be done through a penalty term in the objective function that rewards lower order models. Also, given that the component characteristics in neurological applications are usually known *a priori*, it is advantageous to take such information into account in estimating the model whereby resulting tensors are penalised for their distance from the nearest component. This allows a clear segmentation of the data set as well which can be an important tool in subsequent Fiber tracking.

Conclusions

Two new methods to estimate a diffusion tensor mixture model have been presented and compared to the previous method. While the previous method suffers from restricting assumptions and higher estimation errors, the proposed methods based on differential equation modelling and projection

pursuit based search were found to offer significantly lower estimation error and much faster performance. The differential equation modelling method was found to be the fastest, but suffers from occasional instability that unpredictably causes severe errors in estimation. On the other hand, the method based on projection pursuit was found to be sufficiently fast while maintaining the lowest error rate among all methods. The main advantage of this approach is the elimination of dependence on *a priori* knowledge about the tensor composition, which allows more flexibility in practical applications. The new solution strategy offers a stable method to compute a multi-component model for diffusion tensor imaging data that is optimal in the least-squares sense. Preliminary results from computer simulations as well as experimental data acquired from normal human volunteers seem encouraging and suggest several uses of the new method, including resolving partial volume problems of white matter/gray matter with cerebrospinal fluid as well as sensitivity to detect multiple white matter Fibers.

Acknowledgements

The real data acquired for this work was obtained using the MRI research system of the Biomedical Imaging Technology Center (BITC), Emory/Georgia Institute of Technology Biomedical Engineering Department, Atlanta, Georgia, USA.

References

[1] Le Bihan D, Mangin JF, Poupon C, Clark CA, Pappata S, Molko N, et al. Diffusion tensor imaging: concepts and applications. J Magn Reson Imaging 2001;13(4):534–46.
[2] Torrey HC. Block equations with diffusion terms. Phys Rev 1956;104(3):563–5.
[3] Basser PJ, Jones DK. Diffusion-tensor MRI: theory, experimental design and data analysis – a technical review. NMR Biomed 2002;15(7–8):456–67.
[4] Basser PJ, Mattiello J, LeBihan D. Estimation of the effective self-diffusion tensor from the NMR spin echo. J Magn Reson B 1994;103(3):247–54.
[5] Hsu EW, Buckley DL, Bui JD, Blackband SJ, Forder JR. Two-component diffusion tensor MRI of isolated perfused hearts. Magn Reson Med 2001;45(6):1039–45.
[6] Inglis BA, Bossart EL, Buckley DL, Wirth 3rd ED, Mareci TH. Visualization of neural tissue water compartments using biexponential diffusion tensor MRI. Magn Reson Med 2001;45(4):580–7.
[7] Clark CA, Hedehus M, Moseley ME. Diffusion time dependence of the apparent diffusion tensor in healthy human brain and white matter disease. Magn Reson Med 2001;45(6):1126–9.
[8] Clark CA, Hedehus M, Moseley ME. *In vivo* mapping of the fast and slow diffusion tensors in human brain. Magn Reson Med 2002;47(4):623–8.
[9] Tuch DS, Reese TG, Wiegell MR, Makris N, Belliveau JW, Wedeen VJ. High angular resolution diffusion imaging reveals intravoxel white matter fiber heterogeneity. Magn Reson Med 2002;48(4):577–82.
[10] Beaulieu C. The basis of anisotropic water diffusion in the nervous system – a technical review. NMR Biomed 2002;15(7–8):435–55.
[11] Frank LR. Anisotropy in high angular resolution diffusion-weighted MRI. Magn Reson Med 2001;45(6):935–9.
[12] Frank LR. Characterization of anisotropy in high angular resolution diffusion-weighted MRI. Magn Reson Med 2002;47(6):1083–99.
[13] Basser PJ, Pajevic S, Pierpaoli C, Duda J, Aldroubi A. *In vivo* fiber tractography using DT-MRI data. Magn Reson Med 2000;44(4):625–32.
[14] Mori S, van Zijl PC. Fiber tracking: principles and strategies – a technical review. NMR Biomed 2002;15(7–8):468–80.
[15] Poupon C, Clark CA, Frouin V, Regis J, Bloch I, Le Bihan D, et al. Regularization of diffusion-based direction maps for the tracking of brain white matter fascicles. Neuroimage 2000;12(2):184–95.
[16] Bammer R, Acar B, Moseley ME. *In vivo* MR tractography using diffusion imaging. Eur J Radiol 2003;45(3):223–34.
[17] Lori NF, Akbudak E, Shimony JS, Cull TS, Snyder AZ, Guillory RK, et al. Diffusion tensor fiber tracking of human brain connectivity: acquisition methods, reliability analysis and biological results. NMR Biomed 2002;15(7–8):494–515.
[18] Friedman JH, Stuetzle W. Projection pursuit regression. J Am Stat Assoc 1981;76(376):817–23.
[19] Friedman JH. Exploratory projection pursuit. J Am Stat Assoc 1987;82(397):249–66.
[20] Kadah YM, Ma X, LaConte S, Yassine I, Hu X. Robust multi-component modeling of diffusion tensor magnetic resonance imaging data. Proc SPIE 2005;5746:148–59.
[21] Yassine IA, Youssef AM, Kadah YM. Novel multi-tensor estimation for high-resolution diffusion tensor magnetic resonance imaging. Proceedings of the twenty third national radio science conference (NRSC), March 14–16; 2006. p. 1–12.